DETECTION OF SMALL CONVECTIVE PATTERNS IN OBSERVATIONS AND SIMULATIONS

B. LEMMERER[1], D. UTZ[1], A. HANSLMEIER[1], A. VERONIG[1],
H. GRIMM-STRELE[2], S. THONHOFER[1] and I. PIANTSCHITSCH[1]

[1]*IGAM/Institute of Physics, University of Graz,
Universitätsplatz 5, A–8010 Graz, Austria*
[2]*Institute of Mathematics, University of Vienna,
Nordbergstraße 15, A–1090 Wien, Austria*

Abstract. Recent results from high resolution solar granulation observations indicate the existence of a population of small granular cells on scales below 600 km in diameter, located in the intergranular lanes. We studied a set of Hinode SOT images and high resolution radiation hydrodynamics simulations in order to analyze small granular cells and to study their physical properties. An automated image segmentation algorithm specifically adapted to high resolution simulations for the identification of granules was developed. The algorithm was also used to analyze and compare physical quantities provided by the simulation and the observations. We found that small granules make a distinct contribution to the total area of granules. Both in observations and simulations, small granular cells exhibit on average lower intensities and vertical velocities.

Key words: granulation - Hinode - ANTARES

1.   Introduction

The granulation is a distinct feature of the solar photosphere generated by convection. The recent discovery of a distinct sub-population of granular cells with scales smaller than the dominant scale of 1000 km, has again drawn attention to the topic of the solar granulation, as their formation and dissipation is unclear (Abramenko *et al.* 2012). In this study, we investigate high resolution solar observations and Radiation Hydrodynamics (RHD) simulations in order to identify and analyze small convective patterns. For this purpose, the newly developed segmentation algorithm from Lemmerer *et al.* (2014) was applied to the data.
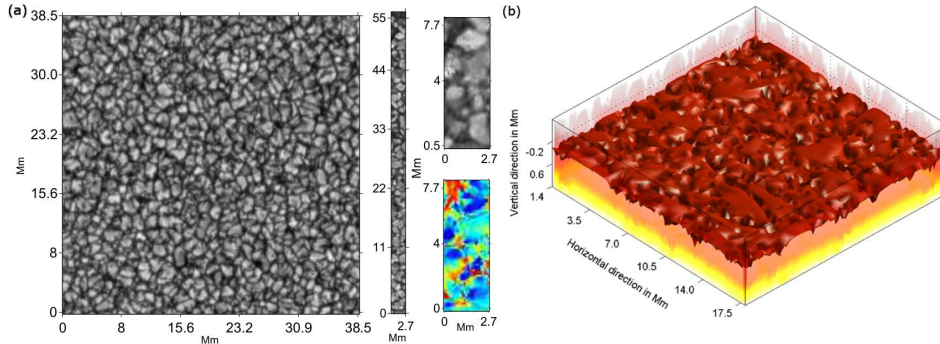
Figure 1: (a; left panel) blue-continuum exposure taken by the SOT/BFI (spatial sampling: 77 km per pixel); (a; middle panel) a slit exposure taken by the SOT/SP; (a; right panel) a detail of the slit exposure and the corresponding line-of-sight velocity profile resulting from the application of the MERLIN inversion code with a sampling of 110 km per pixel. (b) Three-dimensional RHD simulation; the color coded temperature shows the granular pattern on the isosurface of $\tau = 1$.

2. Data

Blue continuum images observed by the Japanese Hinode Solar Optical Telescope (SOT; Tsuneta *et al.* 2008) and RHD simulation data computed with the ANTARES-code (Muthsam *et al.* 2010) were analyzed.

Hinode Data The segmentation algorithm was applied to a selected data set of 108 blue continuum images taken by the SOT/BFI from 2010-05-01 to 2010-07-31, as well as white light exposures taken from the SOT/SP (see Figure 1a). In order to study the vertical velocities of the segmented granules, the line of sight velocities resulting from the application of the MERLIN inversion code to spectropolarimetric data were analyzed (Lites, 2010). For this purpose the segmentation algorithm was applied to an inverted dataset from 2007-01-20 consisting of 29 images (see Figure 1b).

3D Simulations ANTARES (A Numerical Tool for Astrophysical RE-Search) is a RHD code to numerically simulate the solar near-surface convection (box-in-a-star approach; Muthsam *et al.* 2010). The code solves the set of RHD equations using a 5th-order accurate-weighted essentially non-

oscillatory (WENO) numerical scheme. As initial condition for the simulation a 6 Mm wide and 4 Mm deep model is used and was copied three times in each horizontal direction such that the resulting model has a horizontal extent of 18 Mm. The radiative transfer equation in the upper 1.2 Mm of the domain is solved using non-grey opacities with 4 bins. The angular integration is done according to a Gauss-Radau formula with 18 rays (Tanner *et al.*, 2012). The model uses the boundary conditions BC 3b from Grimm-Strele *et al.* (2013) and allows free in- and outflow in the vertical direction.

Figure 1b illustrates the temperature distribution of the 3D model. The horizontal cut at $\tau = 1$ reveals the granular pattern. The simulation box comprises 18 Mm in the horizontal directions and over 7 Mm in the vertical direction. In the horizontal directions the resolution is 35 km.

3. Image segmentation method

The newly developed 2D segmentation algorithm is based on the idea of using multiple thresholds applied to the vertical velocity and incorporating methods of pattern recognition, like edge detection routines and morphological operations applied to the emerging intensity profiles. The whole scheme is a bottom-up approach. Large fragments are sequentially broken down into smaller structures by changing threshold levels. The segmentation itself is done by a recursive thresholding routine, requiring an initial upper threshold as well as a minimum lower threshold as input parameters (Lemmerer *et al.* 2014).

The algorithm can be applied to intensity as well as to vertical velocity profiles. For the thresholding of the RHD and Hinode SOT/SP data we used the vertical velocity and the line of sight velocity from the inverted SP data to obtain a more distinct separation of the structures. In the case of the white light images from the SOT/BFI instrument, intensity images can be processed instead. After finishing the tresholding routine the intensity maps are used for the image-processing operations. The applied image processing steps, plus a labeling of all objects, result in the final segmentation mask, which is then applied to the images in order to extract statistical information of the identified granules (see Figure 2).
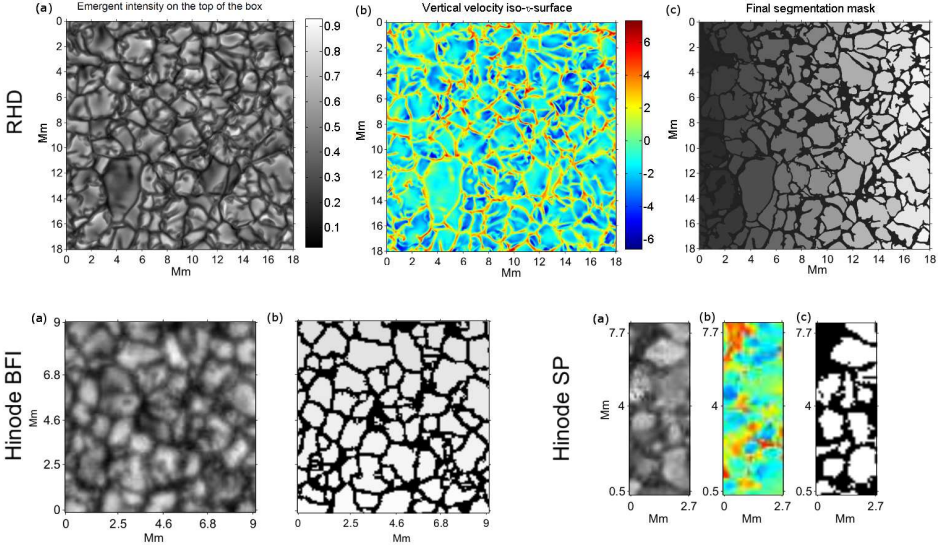
Figure 2: (upper panel) Segmentation algorithm applied to the RHD data: (a) Normalized emergent intensity and (b) vertical velocity profiles (RHD) , (c) final segmentation mask; (lower panel left) algorithm applied to (a) Hinode SOT/BFI white light image and (b) the segmentation result; (lower panel right) application of the algorithm to (a) Hinode SOT/SP blue continuum, (b) line of sight velocity exposures and (c) the segmentation result.

4.   Results

For our analysis of the RHD data we used a two-hour sequence with a temporal resolution of 10 seconds. In Fig. 3, we compare the analysis of the intensity and vertical velocity distributions as well as the structural information of granules derived from RHD data to Hinode BFI and SP data. Figures 3a-c show the mean granular intensity of the simulation, the white light images from the SOT/BFI, and the SOT/SP instrument versus its equivalent diameter. In case of the RHD and the SP data, the intensity increases up to a diameter of 1000 km, indicated by the slope of the 3rd polynomial and linear fits (dashed black and solid black lines). For RHD data, the linear fit indicates a weakly decreasing trend for granules larger than 900 km in diameter. In the intensity distribution derived from the BFI images a linear trend towards higher intensities is visible. The distribution of the mean vertical velocity of the small granules identified (see Fig. 3d,e)
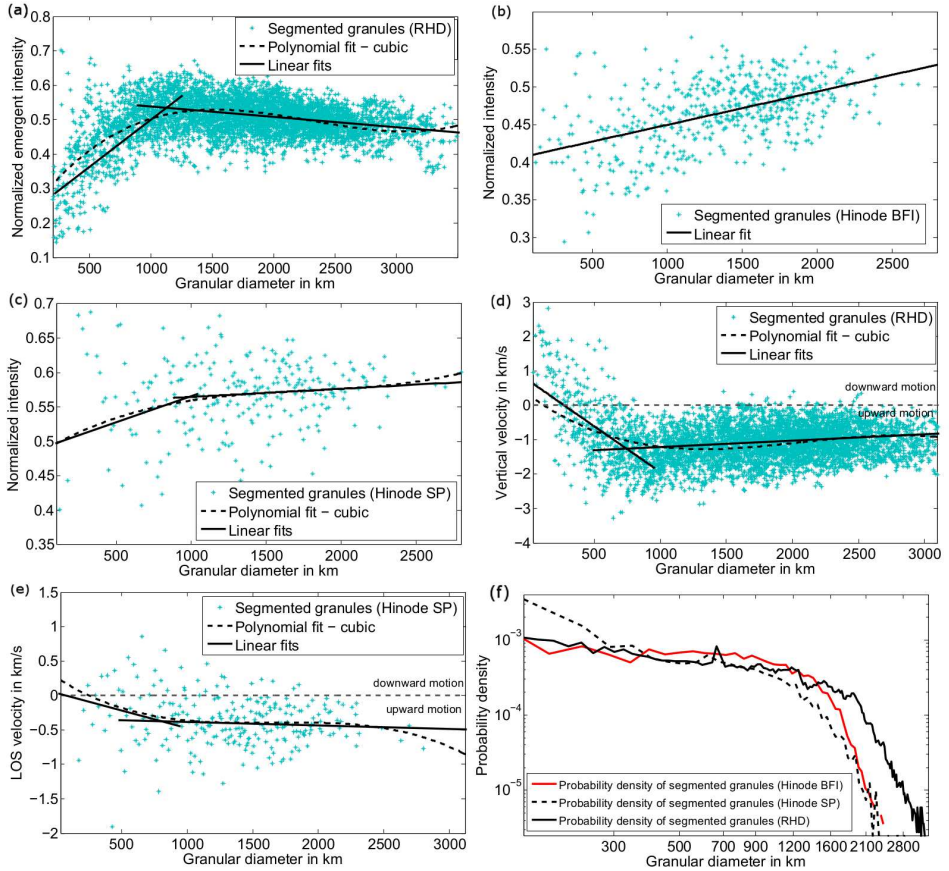
Figure 3: Normalized emergent intensity of granules vs. granular diameter for (a) RHD, (b) Hinode SP data and (c) Hinode BFI data. Scatter plot of granular diameter vs. mean vertical velocity of segmented granules for (d) RHD and (e) Hinode SOT/SP data. (f) The probability density functions for RHD, Hinode SOT/BFI and SOT/SP data.

exhibit a large scatter, which may relate to different stages of their evolution, as they are predominantly found in deeper layers (see Lemmerer *et al.* 2014). The polynomial and linear fits indicate a decrease of vertical velocity (upwards moving plasma) with decreasing granular diameters and are thus strengthening the concept of the existence of two distinct populations. The probability density functions of the equivalent diameters in Fig. 3f show an increase in the number of detected objects towards smaller scales.

5. Summary and conclusions

The analysis of the intensity and the vertical velocity distributions of the identified granules in RHD simulations and Hinode SOT images showed different results for small granules and for granules larger than 1000 km. The fits of the intensity as a function of the granular diameter indicate a positive slope for larger granules. For regular granules a decrease in the slope is visible and small granules feature lower intensities. The analysis of the vertical velocity illustrates a large scatter for small granules. Especially for RHD data, the identified small granules are in a predominantly downflowing state, while large granules show upflowing motions.

To study the origin of these motions, detailed analysis of the temporal evolution of granules will be carried out. A newly developed 2D tracking algorithm will give information about the dynamics of granules regarding their structural variation and the interaction with and development of granular substructures.

6. Acknowledgements

References

Abramenko, V. I., Yurchyshyn, V. B., Goode, P. R., *et al.*: 2012, *Astrophys. J.* **756**, L27.

Grimm-Strele, H., Kupka, F., Löw-Baselli, B., *et al.*: 2013, *New Astronomy*, ArXiv e-prints

Lemmerer, B., Utz, D., Hanslmeier, A. *et al.*: 2014 *Astron. Astrophys.* **563**, 107.

Lites, B., SOT/SP Level2 Data Description

Muthsam, H.J., Kupka, F., Löw-Baselli, B., *et al.*: 2010, *New Astronomy* **15**, 460.

Tanner, J. D., Basu, S., and Demarque, P.: 2012, *Astrophys. J.* **759**, 120.

Tsuneta, S., Ichimoto, K., Kasukawa, Y., *et al.*: 2008, *Solar Phys.* **249**, 167.